



# CHORUS

This is the accepted manuscript made available via CHORUS. The article has been published as:

## Dephasing of Single-Photon Orbital Angular Momentum Qudit States in Fiber: Limits to Correction via Dynamical Decoupling

Manish K. Gupta and Jonathan P. Dowling

Phys. Rev. Applied **5**, 064013 — Published 24 June 2016

DOI: [10.1103/PhysRevApplied.5.064013](https://doi.org/10.1103/PhysRevApplied.5.064013)

# Dephasing of single-photon orbital angular momentum qudit states in fiber – Limits to correction via dynamical decoupling

Manish K. Gupta\* and Jonathan P. Dowling

*Hearne Institute for Theoretical Physics, Department of Physics and Astronomy,  
Louisiana State University, Baton Rouge, Louisiana 70803, USA.*

(Dated: May 23, 2016)

We analytically derive a decoherence model for orbital angular momentum states of a photon in a multimode optical fiber and show that rate of decoherence scales approximately exponentially with  $l^2$ , where  $l$  is the azimuthal mode order. We also show numerically that for large values of  $l$  the orbital angular momentum photon state completely dephases. However for lower values of  $l$  the decoherence can be minimized by using dynamical decoupling to allow for qudit high-bandwidth quantum communication and similar applications.

PACS numbers: 42.50.Tx, 42.79.Sz, 42.50.Ar, 42.25.Kb, 42.25.Lc

## I. INTRODUCTION

For the past few years the quantum information community has been putting a great deal of effort into boosting the bit rate for photonic quantum state transmission by encoding more than one bit per photon. This is done by exploiting multiple temporal, spatial, polarization, and frequency modes of the single photon and then preparing a single photon in a superposition of those modes as a qudit. The number of bits then is  $\log_2 d$ , where  $d$  is the dimension of the qudit. The focus has been on using orbital angular momentum (OAM) modes of the photon, particularly in multimode optical fiber, as a road to high bit rate.

Photons that are OAM eigenstates, originate as a consequence of spatial distribution of optical field intensity and phase [1, 2]. The photon carries an azimuthal phase term  $\exp(il\theta)$  and  $l$  units orbital angular momentum [3]. Such phase dependence is characteristic of either Laguerre-Gaussian or Bessel modes and each of these mode families provides a higher dimensional state space. The most immediate advantage of a large state space is the large alphabet size for quantum communication and hence considerable increase in data capacity. Higher dimensional systems have been known to improve security in quantum cryptography [4] and are required by some quantum network protocols [5] and quantum computation schemes [6] to efficiently solve problems like Byzantine agreement problem [7] and quantum coin tossing [8].

There are several protocols that encode quantum information in the two-dimensional Hilbert space of the photon's spin and exploit the polarization or time-bin degrees of freedom [9, 10]. Physical implementations of one such protocol for quantum key distribution has shown that such an encoding is not optimal for practical applications due to a low bit rate [11]. Information encoding based on the two-dimensional Hilbert space of

photon polarization (or SAM) imposes a limitation on the rate of optical communication. To overcome such limitations the orbital angular momentum (OAM) of light has been proposed that uses the photon's spatial mode structure and allows use of higher-dimensional Hilbert space, or a “qudit” encoding of a photon [12]. This leads to an increased alphabet size and subsequently, increased rate of communication [13–15]. Recent experiments have shown that the classical data-carrying capacity of a terabit per second can be achieved using OAM states of light in an optical fiber [16]. The potential of higher dimensional encoding of quantum information to achieve a higher bit rate can only be achieved if the photon can be protected from the decohering effect of optical index of refraction fluctuation in an optical fiber.

Here we report using a detailed calculation; an analytical model for decoherence caused by the refractive index fluctuation in a multi-mode fiber for an OAM photon state. We show that rate of decoherence is faster for large values of  $l$  and it scales exponentially with  $l^2$ , where  $l$  is azimuthal mode number. We additionally show that such a decoherence can be mitigated to a large extent with a *open-loop* control technique called dynamical decoupling (DD) and we numerically show that OAM photon with small values of  $l$  (up to about 10) can be preserved with a fidelity greater than 99%.

The transverse spatial wave function of a paraxial beam is an eigenstate of OAM and it can be written in cylindrical coordinates as

$$\varphi_{p,l}(r, \theta) = \frac{1}{\sqrt{2\pi}} R_{p,l}(r) \exp(il\theta). \quad (1)$$

The functions  $R_{p,l}(r)$  are a basis for the radial dependence, such as the Laguerre-Gauss functions. They are defined in free space as

$$R_{p,l}(r) = \frac{A}{w(z)} \left( \frac{\sqrt{2}r}{w(z)} \right)^{|l|} L_p^{|l|} \left( \frac{2r^2}{w(z)^2} \right) \times e^{ikr^2/[2R(z)]} e^{i(2p+|l|+1) \tan^{-1}(z/z_R)}, \quad (2)$$

---

\* mgupta3@lsu.edu

where  $w(z) = w_0 \sqrt{1 + (z/z_R)^2}$  is the beam width,  $R(z) = z[1 + (z_R/z)^2]$  is the radius of wave-front curvature, and  $z_R = \frac{1}{2}kw_0^2$  is the Rayleigh range. The quantity  $\tan^{-1}(z/z_R)$  is known as the Gouy phase. These  $R_{p,l}(r)$  functions are modified slightly inside fiber.

Optical fibers have other complex spatial modes but for simplicity, we consider here an OAM photon that is launched in to a multimode optical fiber that is in superposition of  $l$  and  $-l$  states and has the following ket representation

$$|\psi_{pl}\rangle = \frac{1}{\sqrt{2\pi}} R_{p,l}(r) [\exp(i l \theta) |p, l\rangle + \exp(-i l \theta) |p, -l\rangle]. \quad (3)$$

For example, such a state could be used as one code letter of a four-letter code for the BB84 protocol [9]. The other letters would be the negative superposition and the individual  $\pm l$  states. The density matrix for the above input state can be written as

$$\begin{aligned} \hat{\rho}_{\text{in}} &= |\psi_{pl}\rangle \langle \psi_{pl}| \\ &= |R_{p,l}(r)|^2 \begin{pmatrix} 1 & e^{i 2l\theta} \\ e^{-i 2l\theta} & 1 \end{pmatrix}. \end{aligned} \quad (4)$$

## II. NOISE MODEL

In general, the index of refraction fluctuation in an optical fiber can be represented by a series of concatenated, homogeneous segments of length  $\Delta L$  with constant index fluctuation  $\Delta\beta = \frac{\omega(n_l - n_{-l})}{c}$  [17, 18]. When a photon that is in superposition of  $+l$  and  $-l$  propagates through the fiber in  $z$  direction the  $E$ -fields see a slightly different refractive index due to the corkscrew nature of the OAM photon. The photon acquires a phase proportional to the azimuthal mode number  $l$ , since the number of helix surfaces in a fixed volume of fiber is proportional to the helix step length  $\lambda/|l|$ . The two independent index of refraction fluctuations interact with the orbital angular momentum degree of freedom of the photon. The noise operator is given by

$$\begin{aligned} \mathbb{M}_z(\delta\phi_j) &= \begin{pmatrix} e^{i l \frac{\delta\phi_j}{2}} & 0 \\ 0 & e^{-i l \frac{\delta\phi_j}{2}} \end{pmatrix} \\ &= \cos\left(l \frac{\delta\phi_j}{2}\right) \mathbb{I} + i \sin\left(l \frac{\delta\phi_j}{2}\right) \hat{L}_z \\ &= e^{i l \frac{\delta\phi_j}{2} \hat{L}_z} \\ &= \mathbb{R}_z(l \delta\phi_j) \end{aligned} \quad (5)$$

where  $\delta\phi_j = \Delta\beta_j \Delta L$  is the phase angle acquired due to propagation through the  $j^{\text{th}}$  segment of fiber and  $\hat{L}_z = -i \frac{\partial}{\partial \theta}$  is orbital angular momentum operator that generates rotation about  $z$  axis. Laguerre-Gaussian beams are eigenfunction of orbital angular momentum

operator  $\hat{L}_z$ . The output density matrix after the interaction in the  $j^{\text{th}}$  segment is given by

$$\begin{aligned} \hat{\rho}_{j\text{out}} &= \mathbb{M}_z(\delta\phi_j) \hat{\rho}_{\text{in}} \mathbb{M}_z(\delta\phi_j)^\dagger \\ &= |R_{p,l}(r)|^2 \begin{pmatrix} 1 & e^{i(2l\theta + l\delta\phi_j)} \\ e^{-i(2l\theta + l\delta\phi_j)} & 1 \end{pmatrix}. \end{aligned} \quad (6)$$

Now, if we assume that cross-talk between OAM modes is negligible [16], which is a good approximation for linear interactions, then the above density matrix can be rewritten as:

$$\hat{\rho}_{j\text{out}} = |R_{p,l}(r)|^2 \begin{pmatrix} 1 & e^{i l(2\theta + \delta\phi_j)} \\ e^{-i l(2\theta + \delta\phi_j)} & 1 \end{pmatrix}. \quad (7)$$

After passing through the fiber with  $n$  homogeneous concatenated segments the output density matrix is

$$\hat{\rho}_{j\text{out}} = |R_{p,l}(r)|^2 \begin{pmatrix} 1 & e^{i(2l\theta)} \prod_{j=1}^n e^{i(l\delta\phi_j)} \\ e^{-i(2l\theta)} \prod_{j=1}^n e^{-i(l\delta\phi_j)} & 1 \end{pmatrix}. \quad (8)$$

We model the sum of acquired phases  $\{\delta\phi_1, \delta\phi_2, \dots, \delta\phi_n\}$  as random variable  $\hat{\phi}$  with a mean  $\langle \hat{\phi} \rangle = \phi_0$  and a nonzero variance  $\langle \Delta\hat{\phi}^2 \rangle = \Delta\phi^2$ . Here  $\phi_0$  is proportional to  $n$  but  $\Delta\phi^2$  is independent of  $n$ . The factor  $\prod_{j=1}^n e^{\pm i l \delta\phi_j}$  in the off-diagonal term of Eq. 8 can be expressed in terms of mean and variance of random variable  $\hat{\phi}$

$$\begin{aligned} \prod_{j=1}^n e^{\pm i l \delta\phi_j} &= \exp\left[\sum_{j=1}^n (\pm i l \delta\phi_j)\right] \\ &= \exp\left[\left(\pm i l \langle \hat{\phi} \rangle \pm i l \Delta\hat{\phi}\right)\right] \\ &= \exp\left[\pm i l \langle \hat{\phi} \rangle\right] \exp\left[\pm i l \Delta\hat{\phi}\right]. \end{aligned} \quad (9)$$

We then Taylor expand the factor  $\exp[\pm i l \Delta\hat{\phi}]$  of Eq. 9 and take the time average to obtain

$$\begin{aligned} \langle \exp[\pm i l \Delta\hat{\phi}] \rangle &= \left\langle 1 \pm i l \Delta\hat{\phi} - \frac{1}{2} l^2 \Delta\hat{\phi}^2 + \dots \right\rangle \\ &= 1 \pm i l \langle \Delta\hat{\phi} \rangle - \frac{1}{2} l^2 \langle \Delta\hat{\phi}^2 \rangle + \dots \end{aligned} \quad (10)$$

Since the mean of variance is zero in Eq. 10, and average of the variance is  $\langle \Delta\hat{\phi}^2 \rangle = \Delta\phi^2$ , hence we obtain the expression [17, 19]

$$\langle \exp[\pm i l \Delta\hat{\phi}] \rangle = 1 - \frac{1}{2} l^2 \Delta\phi^2 + \dots \approx e^{-\frac{1}{2} l^2 \Delta\phi^2}. \quad (11)$$

The condition that  $l\Delta\hat{\phi}$  is small can always be met for small  $l$  by shortening the lengths of the virtual segments. Using Eq. 11, we can write Eq. 9 as

$$\begin{aligned} \left\langle \prod_{j=1}^n e^{\pm i l \delta\phi_j} \right\rangle &= \left\langle \exp[\pm i l \langle \hat{\phi} \rangle] \right\rangle \left\langle \exp[\pm i l \Delta\hat{\phi}] \right\rangle \\ &= e^{\pm i l \phi_0} e^{-\frac{1}{2} l^2 \Delta\phi^2}. \end{aligned} \quad (12)$$

$$\hat{\rho}_{\text{out}} = |R_{p,l}(r)|^2 \begin{pmatrix} 1 & e^{i l (2\theta + \phi_0)} e^{-\frac{1}{2} l^2 \Delta\phi^2} \\ e^{-i l (2\theta + \phi_0)} e^{-\frac{1}{2} l^2 \Delta\phi^2} & 1 \end{pmatrix}. \quad (13)$$

The state represented by  $\hat{\rho}_{\text{out}}$  is no longer pure due to presence of the dephasing term  $e^{-\frac{1}{2} l^2 \Delta\phi^2}$  in the off-diagonal terms and the rate of decoherence is much faster for larger values of  $l$ .

### III. DYNAMICAL DECOUPLING

Dynamical Decoupling (DD) is inspired by the nuclear magnetic resonance (NMR), where tailored time dependent perturbations are used to control system evolution. It is an open-loop control technique that decouples the system from environmental interactions, where the interaction is pure dephasing. It effectively controls the dynamical evolution of the system while still minimizing the effects of environment.

In DD, a sequence of pulse is applied to the system that is faster than the shortest time scale accessible to the reservoir degree of freedom, such that system-bath coupling is averaged to zero. The simplest pulse sequence that cancels system-environment interaction to first order is known as Carr-Purcell-Meiboom-Gill (CPMG) DD pulse sequence[20, 21]. It is a equidistant two pulse sequence that has been ubiquitously used for decoupling of system from environment.

### IV. NUMERICAL RESULTS

To understand the detrimental effects of noise encountered in the communication channel we numerically study three scenarios. First we analyze the decoherence of free evolving OAM photon in a fiber due to index of refraction fluctuations and then we analyze the effectiveness of open-loop control in preserving the coherence of the qubit, where the system is subjected to external, suitably tailored, space-dependent pulses which do not require measurement. Finally we analyze the impact of large values of quantum number  $l$  on decoherence suppression.

Decoherence of a photonic state has its origin in optical index fluctuation of a fiber that can result from both

And finally, with the expression obtained in Eq. 12, the output density matrix in Eq. 8 can be rewritten as

intrinsic and extrinsic perturbations. We model axially varying index dephasing in an optical fiber of length  $L$  by a series of concatenated, homogeneous segments of length  $\Delta L$  with constant  $\Delta n$  [17, 18, 22]. The index fluctuations across these segments is modeled by generating a set of values according to the Rayleigh distribution, whose probability density function is given as

$$f(x, \sigma) = \frac{x}{\sigma^2} e^{-x^2/(2\sigma^2)}, \quad x \geq 0 \quad (14)$$

where  $\sigma \geq 0$ , is the scale parameter of the distribution, and  $x$  is the distance along the fiber [18, 23]. A noise profile of the fiber is extrapolated from these phase error values. Here we assume that the fiber only exhibits linear index fluctuation as the radial dimension of the fiber is very small.

For our numerical analysis we consider the following input state

$$\begin{aligned} |\psi\rangle &= \frac{1}{\sqrt{2\pi}} [R_{p,l}(r) \exp(i l \theta) |p, l\rangle \\ &\quad + R_{p,-l}(r) \exp(-i l \theta) |p, -l\rangle]. \end{aligned} \quad (15)$$

Since  $R(p, l) = R(p, -l)$ , we can normalize the state and rewrite the ket in matrix notation as:

$$|\psi\rangle = \frac{1}{\sqrt{2}} \begin{pmatrix} e^{i l \phi} \\ e^{-i l \phi} \end{pmatrix}. \quad (16)$$

We first calculate the fidelity of the fiber without any error suppression mechanism in place for a particular length, number of sections, and initial state. The initial state of the photon is allowed to freely evolve through each section of the fiber according to

$$\mathbb{M}_z(\delta\phi_j) = \begin{pmatrix} e^{i l \frac{\delta\phi_j}{2}} & 0 \\ 0 & e^{-i l \frac{\delta\phi_j}{2}} \end{pmatrix}, \quad (17)$$

where,  $\delta\phi_j$  includes the phase error from the Rayleigh distribution. The freely evolved state is then compared with the input state. We use fidelity as a measure of effectiveness in preserving the state of photon and it is defined as

$$\mathcal{F} = |\langle \psi_i | \psi_f \rangle|^2, \quad (18)$$

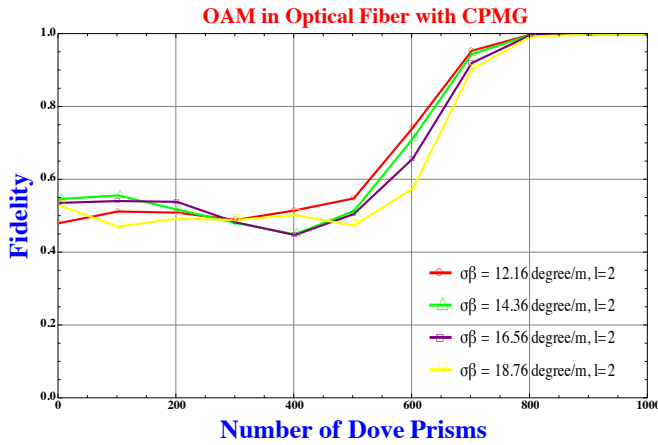


FIG. 1. (Color Online) Fidelity of CPMG sequence in a 500 m optical fiber with perfect pulses. The result shown in the plot is for an OAM state with arbitrary  $\phi$  and  $l = 2$ .

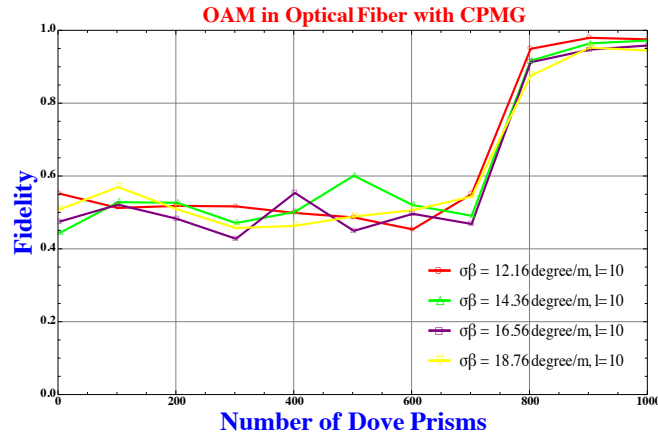


FIG. 2. (Color Online) Fidelity of CPMG sequence in a 500 m optical fiber with perfect pulses. The result shown in the plot is for an OAM state with arbitrary  $\phi$  and  $l = 10$ .

where  $\psi_f$  and  $\psi_i$  represent the final and initial state respectively. The fidelity  $\mathcal{F}$  is averaged over  $n$  fiber noise profiles.

When photon with state of the form Eq. 16 is launched into the fiber of length 500 m it completely dephases and fidelity remains at 50%.

We then calculate fidelity for second scenario where the passive error suppression mechanism called the Carr-Purcell-Meiboom-Gill (CPMG) DD pulse sequence is used for a particular length, number of sections, and initial state [20, 21]. For each section of fiber, the initial state of photon is allowed to freely evolve for a certain distance according to Eq. 17 and then the state is rotated according to the CPMG DD pulse sequence, where the pulse sequence is implemented by inserting a dove prism. This prism is a well-known device in optics that acts as image flipper in one transverse dimension, while leaving unchanged the image in the other transverse dimension [24]. This changes the OAM of a light beam

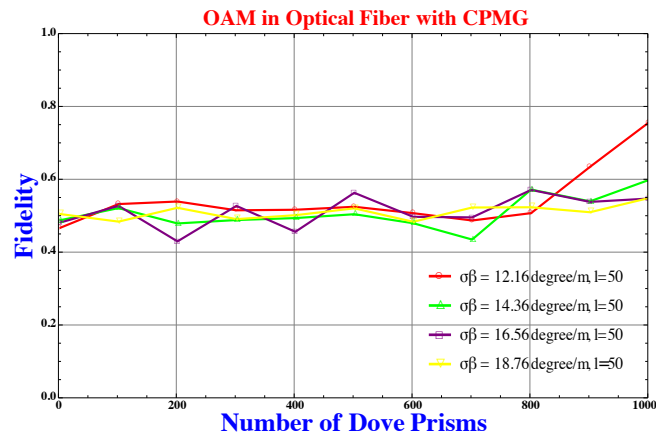


FIG. 3. (Color Online) Fidelity of CPMG sequence in a 500 m optical fiber with perfect pulses. The result shown in the plot is for an OAM state with arbitrary  $\phi$  and  $l = 50$ .

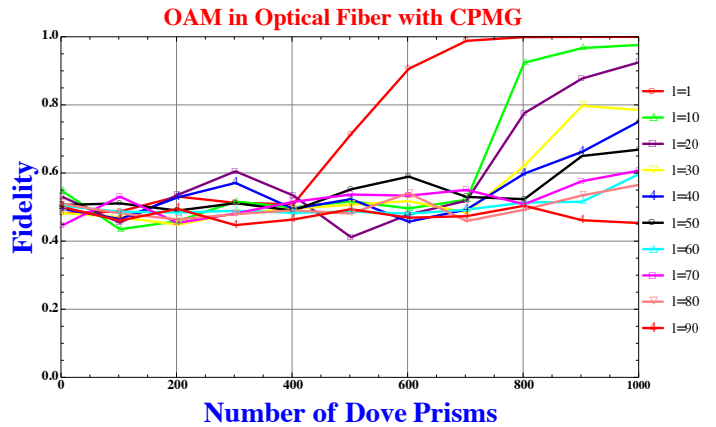


FIG. 4. (Color Online) Fidelity of CPMG sequence in a 500 m optical fiber with perfect pulses. The result shown in the plot is for an OAM state with arbitrary  $\phi$  and  $l$  between one and 100.

from  $l = 1$  to  $l = -1$ . This is repeated for each section in the fiber. We then compare the output state with input state and use fidelity as a measure of effectiveness in preserving the state of photon. We see that for  $l = 2$  the photon state can be preserved with a fidelity greater than 99% as shown in Fig. 1.

Finally we analyze the impact of large quantum number  $l$  on effectiveness of CPMG DD pulse sequence in preserving the OAM state of photon. We find that the fidelity decreases for same number of resource with increasing value of quantum number  $l$  such as  $l = 10$  and  $l = 50$  as shown in Fig. 2 and Fig. 3. As  $l$  is increased from 1 to 100, we see that the DD pulse sequence fails to preserve the OAM state of photon and it completely dephases as shown in the Fig. 4. We note that there is no intuitive relation between the exponential noise scaling and number of prisms.

## V. CONCLUSION

The proposed decoherence model for OAM photons in an optical fiber shows that the rate of decoherence is dependent on  $l^2$ . We then show numerically that the OAM state can be preserved against decoherence caused by the index fluctuation present in a fiber with  $> 99\%$  fidelity using CPMG DD scheme up to a certain maximum value of  $l$ . The DD sequences are implemented with Dove prisms, which presents a practical challenge, and motivates the development of such devices in an integrated optics environment. In realistic scenarios, pulse sequences implemented by Dove prisms may be imperfect but the advantage of CPMG is that it is robust against such pulse error and it can mitigate these errors [17, 25]. For quantum optimal communication schemes, such as quantum key distribution, one would like to put a single-photon into a superposition state of the highest possible number of OAM states. That is because the number of bits per photon scales as  $\log_2(d)$ , where  $d$  is the dimension of the qudit. For example, encoding in a superposition of up to  $p$  and  $l$  OAM states gives

$$d = 2 \frac{(p(p+1))}{2} \frac{(l(l+1))}{2}.$$

Our work here indicates that dephasing will limit  $l_{\max}$  to  $l = 10$  for most scenarios. Dephasing cannot be corrected by DD beyond that value of  $l$ .

A state of the form Eq. 15, which is an equal superposition of OAM  $l$  and  $-l$ , can be prepared by starting with a linear polarized light at  $45^\circ$  and Mach-Zehnder interferometer with quarter-wave plate in both the arms and Dove prism in one of the arms.

We have modeled the effects of index fluctuations on the propagation of the OAM photons in fiber, and show the decoherence scales approximately exponentially with  $l^2$ . We then show that DD sequence may be used to mitigate the decoherence for small  $l$ . Our results then give a road map for using OAM qudit states in fiber.

More generally, our work indicates that there is a path to more generally create passive linear optical elements that can correct dephasing in quantum states of light stored in higher spatial modes including the OAM Laguerre-Gauss modes, and the related Hermite-Gauss and Bessel beam modes. While the current work focuses on the particular example of OAM modes carrying single photons for QKD, a great deal of work has gone into using such states for quantum imaging [26, 27], quantum metrology, quantum sensing [28], and tests of quantum mechanics [29]. Even recently, Zeilinger and collaborators have developed an automated method to search for new experiments that utilize such states [30].

In all such technologies, quantum state dephasing is a limiting factor to the performance of the technology. As we have indicated, one can model dephasing in a fiber as fluctuations in the index of refraction. For remote quantum imaging and sensing applications, the primary source of dephasing is atmospheric turbulence [31]. Our technique outlined in this current paper can be extended to quantum imaging and communications systems where the photon field is recycled through a linear optical device that is designed to implement a dynamical coupling or related scheme to remove the dephasing in any higher order photon mode state.

Our model for decoherence given here is very specific to the use of OAM states in fiber. We realize that there is a great deal of interest in using OAM states for free-space communication but for that regime we will need to develop new model of decoherence and also think carefully about a practical scenario whereby the dynamical decoupling would be implemented in a free-space scenario. Hence we are studying the free-space scenario for future work.

## ACKNOWLEDGMENTS

The authors would like to acknowledge support from the Air Force Office of Scientific Research, the Army Research Office, the National Science Foundation, and the Northrop Grumman Corporation.

- 
- [1] L. Allen, Stephen M. Barnett, and Miles J. Padgett, *Optical Angular Momentum*, edited by Tom Spicer (CRC Press, 2003).
  - [2] David L. Andrews, *Structured Light and Its Applications: An Introduction to Phase-Structured Beams and Nanoscale Optical Forces*, edited by Eric De Cicco (Academic Press, 2008).
  - [3] L. Allen, M. W. Beijersbergen, R. J. C. Spreeuw, and J. P. Woerdman, "Orbital angular momentum of light and the transformation of laguerre-gaussian laser modes," *Phys. Rev. A* **45**, 8185–8189 (1992).
  - [4] Helle Bechmann-Pasquinucci and Asher Peres, "Quantum cryptography with 3-state systems," *Phys. Rev. Lett.* **85**, 3313–3316 (2000).
  - [5] Vahid Karimipour, Alireza Bahraminasab, and Saber Bagherinezhad, "Entanglement swapping of generalized cat states and secret sharing," *Phys. Rev. A* **65**, 042320 (2002).
  - [6] Stephen D. Bartlett, Hubert de Guise, and Barry C. Sanders, "Quantum encodings in spin systems and harmonic oscillators," *Phys. Rev. A* **65**, 052316 (2002).
  - [7] Matthias Fitz, Nicolas Gisin, and Ueli Maurer, "Quantum solution to the byzantine agreement problem," *Phys. Rev. Lett.* **87**, 217901 (2001).
  - [8] Andris Ambainis, "A new protocol and lower bounds for quantum coin flipping," *Journal of Computer and System*

- Sciences **68**, 398 – 416 (2004), special Issue on {STOC} 2001.
- [9] C.H. Bennett and G. Brassard, “Quantum cryptography: Public key distribution and coin tossing,” in *Proceedings of the IEEE International Conference on Computers, Systems, and Signal Processing* (1984).
- [10] Artur K. Ekert, “Quantum cryptography based on bell’s theorem,” *Phys. Rev. Lett.* **67**, 661–663 (1991).
- [11] A. R. Dixon, Z. L. Yuan, J. F. Dynes, A. W. Sharpe, and A. J. Shields, “Continuous operation of high bit rate quantum key distribution,” *Applied Physics Letters* **96**, 161102 (2010).
- [12] S. Etcheverry, G. Canas, E. S. Gomez, W. A. T. Nogueira, C. Saavedra, G. B. Xavier, and G. Lima, “Quantum key distribution session with 16-dimensional photonic states,” *Sci. Rep.* **3** (2013).
- [13] Gabriel Molina-Terriza, Juan P. Torres, and Lluís Torner, “Management of the angular momentum of light: Preparation of photons in multidimensional vector states of angular momentum,” *Phys. Rev. Lett.* **88**, 013601 (2001).
- [14] H. Bechmann-Pasquinucci and W. Tittel, “Quantum cryptography using larger alphabets,” *Phys. Rev. A* **61**, 062308 (2000).
- [15] Simon Groblacher, Thomas Jennewein, Alipasha Vaziri, Gregor Weihs, and Anton Zeilinger, “Experimental quantum cryptography with qutrits,” *New Journal of Physics* **8**, 75 (2006).
- [16] Nenad Bozinovic, Yang Yue, Yongxiong Ren, Moshe Tur, Poul Kristensen, Hao Huang, Alan E. Willner, and Siddharth Ramachandran, “Terabit-scale orbital angular momentum mode division multiplexing in fibers,” *Science* **340**, 1545–1548 (2013).
- [17] Manish K. Gupta, Erik J. Navarro, Todd A. Moulder, Jason D. Mueller, Ashkan Balouchi, Katherine L. Brown, Hwang Lee, and Jonathan P. Dowling, “Preserving photon qubits in an unknown quantum state with knill dynamical decoupling: Towards an all optical quantum memory,” *Phys. Rev. A* **91**, 032329 (2015).
- [18] M. Wulpart, P. Megret, M. Blondel, A.J. Rogers, and Y. Defosse, “Measurement of the spatial distribution of birefringence in optical fibers,” *Photonics Technology Letters, IEEE* **13**, 836–838 (2001).
- [19] Bhaskar Roy Bardhan, Kebei Jiang, and Jonathan P. Dowling, “Effects of phase fluctuations on phase sensitivity and visibility of path-entangled photon fock states,” *Phys. Rev. A* **88**, 023857 (2013).
- [20] S. Meiboom and D. Gill, “Modified spin-echo method for measuring nuclear relaxation times,” *Review of Scientific Instruments* **29**, 688–691 (1958).
- [21] Lorenza Viola, Emanuel Knill, and Seth Lloyd, “Dynamical decoupling of open quantum systems,” *Phys. Rev. Lett.* **82**, 2417–2421 (1999).
- [22] Bhaskar Roy Bardhan, Petr M. Anisimov, Manish K. Gupta, Katherine L. Brown, N. Cody Jones, Hwang Lee, and Jonathan P. Dowling, “Dynamical decoupling in optical fibers: Preserving polarization qubits from birefringent dephasing,” *Phys. Rev. A* **85**, 022340 (2012).
- [23] X. Rong Li, *Probability, Random Signals, and Statistics* (CRC Press, 1999).
- [24] N. González, G. Molina-Terriza, and J. P. Torres, “How a dove prism transforms the orbital angular momentum of a light beam,” *Opt. Express* **14**, 9093–9102 (2006).
- [25] Alexandre M. Souza, Gonzalo A. Álvarez, and Dieter Suter, “Robust dynamical decoupling,” *Philosophical Transactions of the Royal Society of London A: Mathematical, Physical and Engineering Sciences* **370**, 4748–4769 (2012).
- [26] Néstor Uribe-Patarroyo, Alberto Alvarez-Herrero, and Tomás Belenguer, “Measurement of the quantum superposition state of an imaging ensemble of photons prepared in orbital angular momentum states using a phase-diversity method,” *Phys. Rev. A* **81**, 053822 (2010).
- [27] David S. Simon and Alexander V. Sergienko, “Two-photon spiral imaging with correlated orbital angular momentum states,” *Phys. Rev. A* **85**, 043825 (2012).
- [28] Zhang Yuan-Ying Chen Li-Xiang, “Research progress on preparation, manipulation, and remote sensing applications of high-order orbital angular momentum of photons,” *Acta Physica Sinica* **64**, 164210 (2015).
- [29] Alois Mair, Alipasha Vaziri, Gregor Weihs, and Anton Zeilinger, “Entanglement of the orbital angular momentum states of photons,” *Nature* **412**, 313–316 (2001).
- [30] Mario Krenn, Mehul Malik, Robert Fickler, Radek Lapkiewicz, and Anton Zeilinger, “Automated search for new quantum experiments,” *Phys. Rev. Lett.* **116**, 090405 (2016).
- [31] Yongxiong Ren, Guodong Xie, Hao Huang, Long Li, Nisar Ahmed, Yan Yan, Martin P. J. Lavery, Robert Bock, Moshe Tur, Mark A. Neifeld, Robert W. Boyd, Jeffrey H. Shapiro, and Alan E. Willner, “Turbulence compensation of an orbital angular momentum and polarization-multiplexed link using a data-carrying beacon on a separate wavelength,” *Opt. Lett.* **40**, 2249–2252 (2015).